Journal of The Electrochemical Society, **154** (2) A146-A149 (2007)
0013-4651/2006/154(2)/A146/4/$20.00 © The Electrochemical Society

High-Rate Lithium Ion Batteries with Flat Plateau Based on Self-Nanoporous Structure of Tin Electrode

Eiji Hosono,[a] Hirofumi Matsuda,[a] Itaru Honma,[a] Masaki Ichihara,[b] and Haoshen Zhou[a,z]

[a]*National Institute of Advanced Industrial Science and Technology, Energy Technology Research Institute, Tsukuba 305-8568, Japan*
[b]*Material Design and Characterization Laboratory, Institute for Solid State Physics, University of Tokyo, Kashiwa, Chiba 277-8581, Japan*

Tin film as a negative electrode in Li-ion secondary batteries with a flat plateau in the potential vs charge relationship even at a high rate (high current density) were fabricated. The self-nanoporous structure, which means that electrode becomes nanoporous after charge/discharge cycling, due to the lithium insertion/extraction during high-rate charge/discharge, high lithium diffusion coefficients, and metallic conductivity based on tin and tin–lithium alloy, are suitable for the high-rate property. The flat plateau of charge/discharge behavior indicates that this lithium storage device is not a super-capacitor but a secondary battery. This is the first report of a high-rate lithium secondary battery with a flat plateau.
 [DOI: 10.1149/1.2405727]

Manuscript submitted May 30, 2006; revised manuscript received September 26, 2006.
Available electronically December 27, 2006.

Lithium-ion storage devices have been widely studied for possible application in electric devices, especially for mobile or portable electric devices and electric vehicles, which require high energy density and high power density. The synthesis of electrode materials for lithium-ion storage devices with high specific capacity at high charge/discharge current rate has been expected because lithium-ion storage devices with high specific capacities (=high energy density) and high current densities (=high power density) are necessary for industrial use. Many papers have reported materials with only high specific capacities, using nanocrystalline transition metal oxides[1,2] or the alloy reaction such as Si[3,4] and Sn.[5-10] Recently, reports of electrodes with both high specific capacities and high current densities have increased.[11-15] However, high energy and high power lithium-ion secondary batteries with a flat plateau of the charge/discharge curves have not been reported.

Generally, there are the following four problems which arise due to the nature of lithium-ion batteries or lithium storage devices, which need to be solved in order to develop high rate lithium storage devices: (*i*) increasing the electronic conductivity of the electrode materials by using highly conductive materials, (*ii*) reducing the required diffusion length in the active materials by decreasing the particle size, (*iii*) reducing the effective specific current density by high surface area, and (*iv*) realizing high cycle performance by nanoparticles and porous structure to ease the tension caused by volume expansion upon insertion of the lithium.

In our recent work, lithium storage devices with both high power and energy densities by fabricating a nanocrystalline and mesoporous metal oxide film on a nickel mesh, knitted of nickel micrometer-wires via the self-template method, are reported.[11,12] The novel structure partly mitigates the above four problems and enables a high specific capacity to be obtained at a high charge/discharge current rate. However, the thickness of the metal oxide layer on the Ni micrometer wire should be less than several hundred nanometers. The thickness of the metal oxide layer cannot be increased in order to obtain high electronic conductivity because the resistivity of metal oxide (NiO[11] or Fe_2O_3[12]) is high. Hence, the weight ratio of active materials is very small. Moreover, the greatest weakness of high-rate lithium storage devices reported so far is the profile of the charge/discharge potential curve, which is a capacitor-like curve at the high-rate charge/discharge condition.[8,11-15] In the capacitor-like curves, the charge/discharge curves show no potential flat plateaus and a linear decrease/increase of the potential in accordance with the lithium insertion/extraction. Hence, the reported devices cannot be called high-rate lithium-ion secondary batteries but should rather be called high-rate lithium storage devices or supercapacitors. Such high-rate lithium storage devices or super-capacitors cannot satisfy industrial needs, so there is a need to develop high-rate lithium-ion secondary batteries with potential flat plateaus in the charge/discharge process.

Here, the metallic tin on SUS-304 mesh is used as a negative electrode for the high-rate lithium-ion secondary batteries with potential flat plateaus, which are fabricated by electrodeposition, because tin has a high theoretical capacity of 994 mAh/g and high electronic conductivity based on the metallic conductivity and high diffusion coefficient of Li–Sn alloy of 10^{-7}–10^{-8} cm^{-2} s^{-1},[16] which is over 1000 times the diffusion coefficient of general metal oxide electrodes of 10^{-10}–10^{-17} cm^{-2} s^{-1}.[13,17] So, there are not only four problems to be solved for high-rate lithium-ion batteries; a fifth problem is how to increase the lithium-ion diffusion coefficient in active materials to decrease the diffusion polarization in the high-rate charge/discharge process. This paper is the first to report the synthesis of nanoporous metal tin as an anodic electrode for high-rate lithium-ion secondary batteries with a flat plateau and good cycle performance. The properties of the high-rate secondary batteries of metallic tin include good metallic conductivity, high lithium-ion diffusion coefficient, and self-porous reaction process due to the lithium insertion/extraction by high-rate charge/discharge.

Experimental

A precursor solution was prepared by dissolving $SnCl_2 \cdot 2H_2O$ (99.9% purity, Wako Pure Chemicals Co., Ltd., Japan) in H_2O with HCl (99.9% purity, Wako Pure Chemicals Co., Ltd., Japan), which was added dropwise to the solutions to adjust pH values (about 0.9). The concentration of the tin ions was fixed at 0.0075 mol dm^{-3}.

The cell for deposition was a conventional three-electrode cell in which a Pt(200 nm)/Ti/glass plate was used as counter electrode with separation from the working electrode of SUS-304 (100 mesh) for tin deposition. A saturated calomel electrode (SCE) was used as the reference electrode. A constant potential of −2.0 V was applied to the SUS-304 for 5 min in the precursor solution. The deposited tin film was rinsed by deionized water and dried at room temperature in the vacuum condition.

Electrochemical measurements were carried out using the three electrodes set up in a twin beaker cell connected with a microcapillary acting as the separator. The fabricated tin film on the mesh was used as the working electrode. The reference and counter electrode were prepared by spreading and pressing of lithium metals on the SUS-304 mesh (100 mesh). A 1 mol dm^{-3} $LiClO_4$ in ethylene carbonate (EC)/diethyl carbonate (DEC) was used as electrolyte. Cell

[z] E-mail: hs.zhou@aist.go.jp

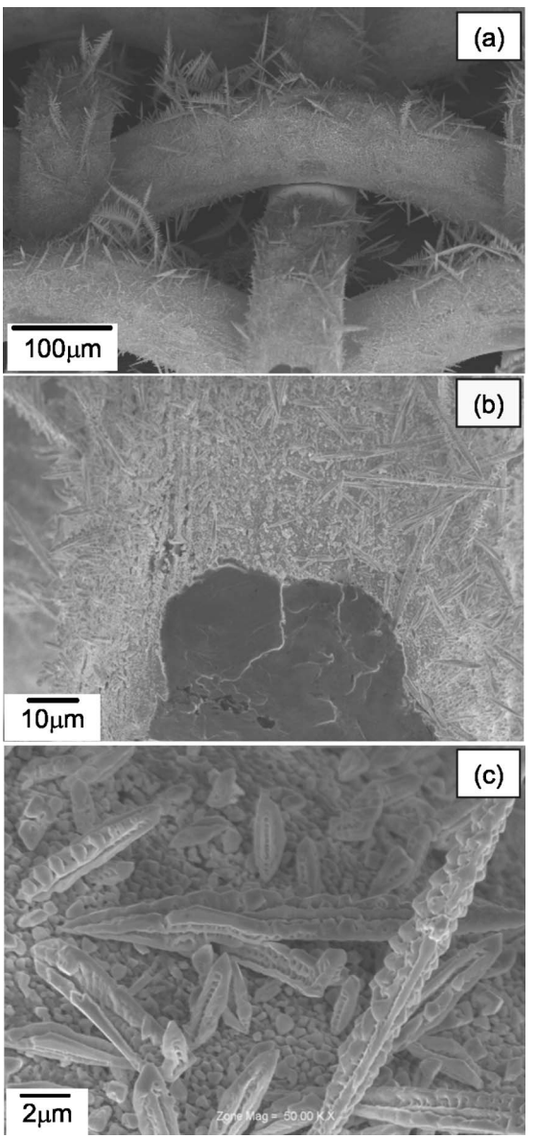

Figure 1. SEM images of the tin films on SUS-304 fabricated by the electrodepostion at −2.0 V (vs SCE) for 5 min.

assembly was carried out in a glove box under an argon atmosphere. The charge/discharge performance of the materials was investigated in such a three-electrode cell using lithium metal as counter and reference electrodes. The weight in specific capacity (mAh/g) and current rate (A/g) was calculated by only active materials. The charge/discharge performance was measured at various current densities of 0.1, 1, 10, and 20 A/g. The potential window at the low-rate condition (0.1 and 1 A/g) and at the high-rate condition (10 and 20 A/g) was 0.01–0.8 and 0.01–1.5 V, respectively.

Results and Discussion

Figure 1 shows the electrodeposited tin film on the SUS-304 mesh. The tin dendrite grown on the SUS-304 can be seen in the low magnification images in Fig. 1a and b. The length of tin dendrite is around several tens of micrometers. Figure 1c shows tin particles with sizes ranging from several hundred nanometers to several micrometers; thus, each dendrite is not a nanostructure but a microstructure. The morphology of each dendrite is similar to that of electrodeposited dendrite.[18]

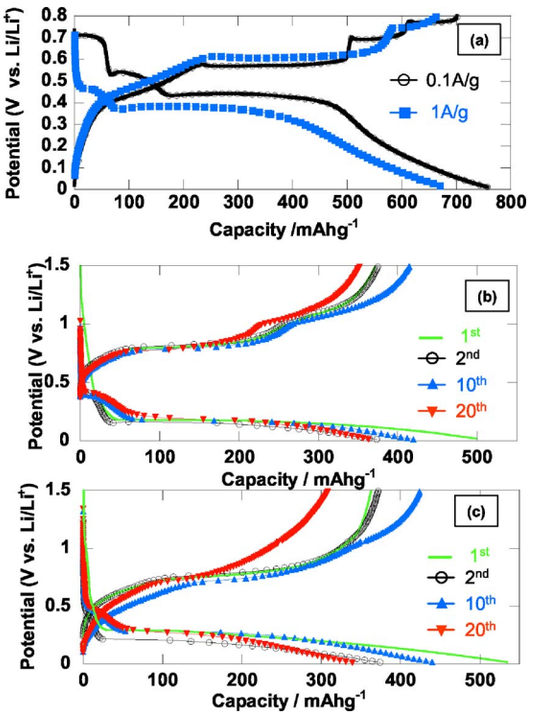

Figure 2. (Color online) (a) Constant current discharge/charge curves of the 2nd cycle at 0.1 and 1.0 A/g and (b and c) constant current discharge/charge curves at 10 and 20 A/g, respectively. Those were recorded in 1 mol dm^{-3} $LiClO_4$ in EC/DEC electrolyte.

The properties of the lithium-ion secondary batteries using tin anodes were tested via constant current charge/discharge measurement. Figure 2a shows the second charge/discharge cycling curves performed at 0.1 and 1 A/g over the voltage range of 0.01–0.8 V vs a Li/Li^+ reference electrode. In the curves at 0.1 A/g, the discharge

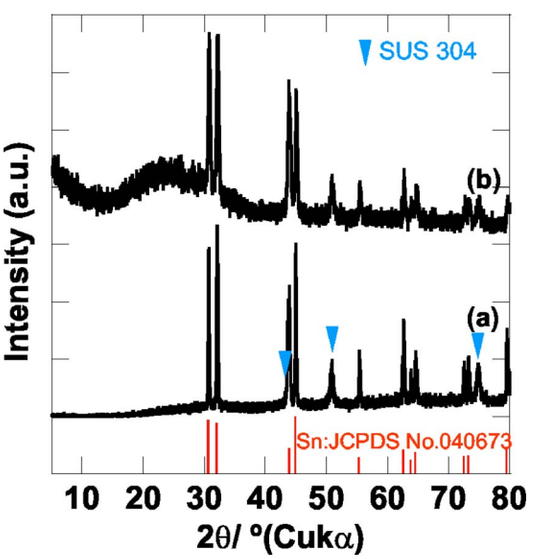

Figure 3. (Color online) (a) XRD patterns of the tin film before the charge/discharge measurement and (b) after the 21st cycle charge/discharge measurement at 10 A/g.

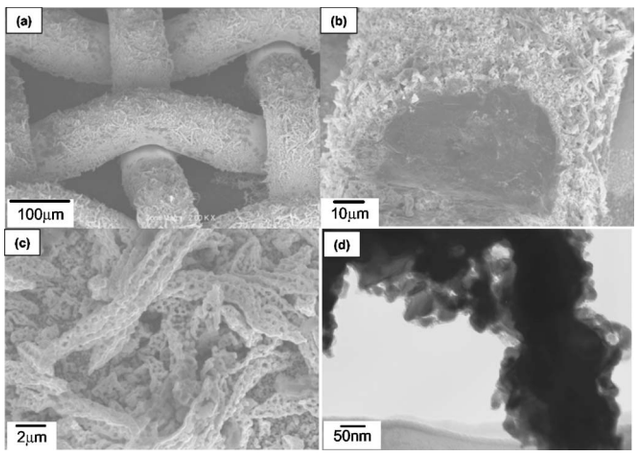

Figure 4. (a–c) SEM images and (d) TEM image of the porous tin film after the 21st cycle charge/discharge measurement at 10 A/g.

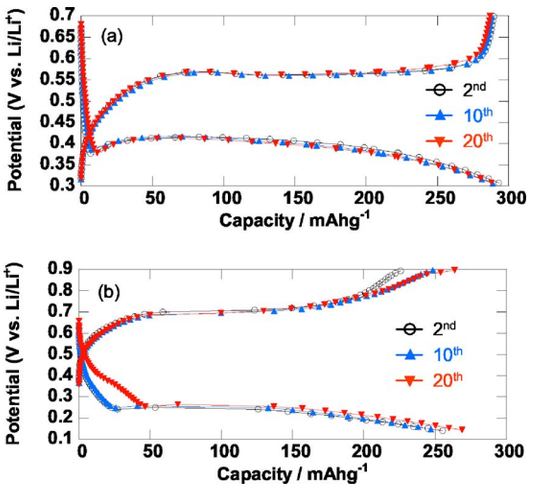

Figure 5. (Color online) (a) Constant current discharge/charge curves at 1.0 A/g over the voltage range of 0.3–0.7 V vs a Li/Li^+ reference electrode and (b) constant current discharge/charge curves at 20 A/g over the voltage range of 0.9–0.14 V vs a Li/Li^+ reference electrode.

curve indicates three plateaus from 0.7 to 0.4 V. After the third plateau, the curve gradually decreases to 0.01 V. The discharge curve is similar to that reported previously.[7]

The first plateau at 0.7 V is the reaction

$$Sn \rightarrow Li_{0.4}Sn \quad [1]$$

The second plateau at around 0.55 V is the reaction

$$Li_{0.4}Sn \rightarrow LiSn \quad [2]$$

The third plateau at around 0.4 V is the reaction

$$LiSn \rightarrow Li_{7/3}Sn \quad [3]$$

The gradual decreasing curve is the reaction

$$Li_{7/3}Sn \rightarrow Li_{2.5}Sn \rightarrow Li_{2.6}Sn \rightarrow Li_{3.5}Sn \rightarrow Li_{4.4}Sn \quad [4]$$

In this case, the capacity of the second cycle at 0.1 A/g is about $Li_{3.5}Sn$.

It is considered that the typical lithium insertion reaction is caused by this electrodeposited tin film on SUS-304 because the discharge curve clearly shows almost all of Reactions 1-4. In the charge/discharge curves at the relatively high rate of 1.0 A/g, the plateau at 0.7 V in discharge, which is observed in the cycling curves at 0.1 A/g, is converted into the drastic decreasing curve with lithium insertion, like a capacitor. The large capacity of around 680 mAh/g includes the plateau length with 250–300 mAh/g at 0.4 V in discharge, corresponding to the lithium insertion from LiSn–$Li_{7/3}Sn$, which is similar to that in the cycling curves at 0.1 A/g. Here, the cycle performance such as the 20th cycle is poor due to the large volume change of the lithium insertion from Sn to $Li_{4.4}Sn$.[7]

Figures 2b and c show the charge/discharge cycling curves performed at the high rate of 10 and 20 A/g over the voltage range of 0.01–1.5 V vs a Li/Li^+ reference electrode, respectively. Taking into account the overpotential due to the increase of current density resulting in the change of voltage range, the plateaus at 0.4 V in the discharge curve at the low rate (0.1 A/g) decrease to 0.15 V in both the 10 and 20 A/g curves. The first and second plateaus at 0.7 and 0.55 V in the cycling curves at 0.1 A/g in Fig. 2a are converted into the capacitor-like curve. The curves from the second cycle to 20th cycle at 10 and 20 A/g indicate good cycle performance. Each discharge capacity shows a large capacity of around 350–400 mAh/g, which is similar to that of graphitic carbon, in spite of the very-high-rate condition. Moreover, the most important characteristic is the stable plateau, which is derived from the reaction of LiSn $\rightarrow$ $Li_{7/3}Sn$ at around 0.15 V at the high-rate condition of 10 and 20 A/g. The plateau length with around 250 mAh/g still remains, which is near to 300 mAh/g at the low-rate condition of 0.1 A/g. The theoretical capacity of LiSn $\rightleftharpoons$ $Li_{7/3}Sn$ is 301 mAh/g. Hence, the flat plateau capacity of around 250 mAh/g even at high rates such as 10 and 20 A/g is near to the theoretical capacity. This flat plateau with good cycle performance at the high-rate condition is suitable for high-rate secondary batteries. In many reports, tin-based intermetallic compounds such as Cu–Sn[9,19] and Sb–Sn[6] were used for the anode electrode because of the poor cyclability of pure tin due to the large volume change.[7] However, our results show that the pure tin anode electrode had good cycle performance at the high-rate condition.

First, we discuss the flat plateau at the high-rate condition. It is considered that solving problems 1, 2, 3, and 5, which is the use of materials having high lithium-ion diffusion coefficients, results in good charge/discharge curves. The solution of problem 1, which is electron conductivity, is confirmed from the X-ray diffraction (XRD) patterns (Fig. 3) of the electrodeposited tin film before charge/discharge measurement and after the 21st cycle at 10 A/g. Judging from the XRD patterns, which indicate the metallic tin pattern, the metallic tin is maintained after the lithium insertion/extraction reaction. The active material is always metallic during the charge/discharge from start to end because the mechanism of lithium storage for the tin electrode is the tin-lithium alloy reaction.[7] The maintenance of the metallic conductivity is suitable for high-rate lithium-ion cells. The solution of problems 2 and 3 based on nanostructure is confirmed by the scanning electron microscopy (SEM) and transmission electron microscopy (TEM) images of the tin films before and after the 21st cycle at 10 A/g in Fig. 1 and 4, respectively. From the low magnification image in Fig. 4a and b, the dendrite is not removed from the SUS-304 mesh. The thickness of the tin film is around 5–10 μm (Fig. 4b), which is thicker than that before charge/discharge as shown in Fig. 1b. As compared with the SEM images between Fig. 1c and 4c, the dendrite tin film is converted into the nanoporous structure. The self-nanoporous reaction based on the volume-change reaction of Li–Sn alloy as shown in Fig. 4c results in increased film thickness. The thickness of 5–10 μm is much larger than the thickness of metal oxides[11,12] on Ni wire for high-rate lithium-ion storage devices. This nanoporous structure is constructed by the nanoparticles as shown in TEM images in Fig. 4d. This nanoporous structure, which is created by self-reaction in the high-rate insertion/extraction based on the volume change reaction of Li–Sn alloy, decreases the required diffusion length in the active materials and the effective specific current den-

Table I. Comparison of the capacity in the limited potential range as the lithium-ion secondary batteries. We use the ratio of capacity in per potential unit, which is defined as $C'/\Delta V$, to estimate the lithium storage device and supercapacitor, here C' is the capacity and ΔV is the limited potential range.

Material (Ref.)	Rate (Ag^{-1})	Current in the cell (mA)	C' in limited region (mAh/g^{-1})	ΔV (V)	$C'/\Delta V$ (mAh/g^{-1} V^{-1})	Classify
This work	10.0	15.1	332	0.15–0.01 V	2370	Secondary batteries
	20.0	19.0	350	0.20–0.01 V	1842	
TiO_2–P_2O_5–SnO_2 CGMN[15]	10.0	10.0	225	1.8–1.0 V	280	Supercapacitor
c-SWNT/TiO_2(TTB-acac)[14]	6.72	—	60	1.7–1.4 V	200	Supercapacitor
SnO_2 nanofibers[8]	23.7	1.9	560	0.9–0.34 V	1000	Supercapacitor
Ni/NiO[11]	10	8	540	1.3–0.5 V	675	Supercapacitor
Ni/Fe_2O_3[12]	13	11	700	1.0–0.01 V	707	Supercapacitor

sity. The solution of problem 5 is based on the high lithium-ion diffusion coefficient of Li–Sn alloy. The lithium-ion diffusion coefficient of $1.8–5.9 \times 10^{-7}$ cm^2 s^{-1} of $Li_{7/3}Sn$ is extremely large.[16] Previous reports[8,11-15] on high-rate lithium storage devices did not consider the use of materials with high lithium-ion diffusion coefficients. Moreover, the electronic conductivity of the active materials in the reports was lower than our metallic conductivity because the other materials were metal oxides. In this work, the electronic conductivity and lithium-ion diffusion coefficient are vastly improved, thus attaining the flat plateau at the high-rate condition.

Second, the solution of problem 4, which is cycle performance, at the high-rate condition is discussed. In a previous study using a tin electrode,[7] the cycle performance was very poor due to the large volume change of the reaction $Sn \rightleftharpoons Li_{4.4}Sn$. In this work, the plateau of the reaction of $LiSn \rightleftharpoons Li_{7/3}Sn$ is focused. The reaction indicates a long theoretical plateau because the reaction has the largest lithium-storage reaction of 4/3 lithium (301 mAh/g) per unit in the seven reactions as shown in Eq. 1-4. If the lithium-storage reaction is not $Sn \rightleftharpoons Li_{4.4}Sn$ but $Sn \rightleftharpoons Li_{7/3}Sn$, the volume change is greatly decreased. In fact, the charge/discharge cycling curves performed at 1 A/g over the voltage range of 0.3–0.7 V vs a Li/Li^+ reference electrode indicate nearly perfect cycle performance as shown in Fig. 5a because the reaction of $LiSn \rightleftharpoons Li_{7/3}Sn$ is only occurred in the windows of 0.3–0.7 V judging from Fig. 2a. In the case of the high-rate condition, the plateau of $LiSn \rightleftharpoons Li_{7/3}Sn$ at 0.4 V in the discharge process in the case of low rate (0.1 A/g) is decreased to 0.15 V due to the overpotential. It is considered that other lithium storage potentials of $Li_{7/3}Sn \rightarrow Li_{2.5}Sn \rightarrow Li_{2.6}Sn \rightarrow Li_{3.5}Sn \rightarrow Li_{4.4}Sn$ are also decreased to less than 0.0 V vs Li/Li^+ resulting from overpotential at the high-rate condition. The capacity at the low-rate condition of 0.1 A/g after the cycling of 10 times at high-rate condition of 20 A/g is larger than that of 20 A/g after 10 cycling and similar to the that of 0.1 A/g as shown in Fig. 2a. Therefore, the amount of stored lithium per unit is not 4.4 but near 7/3. This small volume change based on the storage of 7/3 lithium caused the good cycle performance. When the potential window is more decreased such as 0.9–0.14 V vs a Li/Li^+ reference electrode at the high-rate condition of 20 A/g, the charge/discharge cycling curves indicate good cycle performance as shown in Fig. 5b.

In Table I, the specific capacity in the limited voltage regions among this work and other reported works for high-rate lithium-ion storage devices are compared. Other works have not shown the flat plateau. Hence, the $C'/\Delta V$ of 2370 mAh/g^{-1} V^{-1} in our work is much larger than those of other works and the range of voltage change ΔV (0.14 V) is very small. The $C'/\Delta V$ of about 1000 mAh/g^{-1} V^{-1} of SnO_2 nanofiber is also relatively high.[8] However, the absolute current of 1.9 mA[8] in the cell for 23.7 A/g is much smaller than those of other works due to the very small amount of active materials. From Table I, only our device can be called a lithium-ion secondary battery.

Conclusions

Electrodeposited tin dendrite indicates a large capacity of 420 mAh/g (10th cycle) based on the large flat plateau at high current densities of 10 and 20 A/g. The metallic electron conductivity, high lithium-ion diffusion coefficients, and self-nanoporous structure of tin during high-rate charge/discharge due to tin–lithium alloy are suitable for the flat plateau at the high-rate condition. Moreover, the small volume change based on the Sn–$Li_{7/3}Sn$ reaction results in good cycle performance. The lithium-ion batteries based on this metallic tin as the negative electrode are not super-capacitors but real high-rate lithium secondary batteries with a flat plateau and good cycle performance.

National Institute of Advanced Industrial Science and Technology assisted in meeting the publication costs of this article.

References

1. P. Poizot, S. Laruelle, S. Grugeon, L. Dupont, and J. M. Tarascon, *Nature (London)*, **407**, 496 (2000).
2. X. Wang, X. Chen, L. Gao, H. Zheng, Z. Zhang, and Y. Qian, *J. Phys. Chem. B*, **108**, 16401 (2004).
3. B. Gao, S. Sinha, L. Fleming, and O. Zhou, *Adv. Mater. (Weinheim, Ger.)*, **13**, 816 (2001).
4. W. J. Weydanz, M. Wohlfahrt-Mehrens, and R. A. Huggins, *J. Power Sources*, **81–82**, 237 (1999).
5. Y. Idota, T. Kubota, A. Matsufuji, Y. Maekawa, and T. Miyasaka, *Science*, **276**, 1395 (1997).
6. J. Yang, Y. Takeda, N. Imanishi, and O. Yamamoto, *J. Electrochem. Soc.*, **146**, 4009 (1999).
7. M. Winter and J. Besenhard, *Electrochim. Acta*, **45**, 31 (1999).
8. N. Li and C. R. Martin, *J. Electrochem. Soc.*, **148**, A164 (2001).
9. N. Tamura, R. Ohshita, M. Fujimoto, S. Fujitani, M. Kamino, and I. Yonezu, *J. Power Sources*, **107**, 48 (2002).
10. S. D. Beattie, T. Hatchard, A. Bonakdarpour, K. C. Hewitt, and J. R. Dahn, *J. Electrochem. Soc.*, **150**, A701 (2003).
11. E. Hosono, S. Fujihara, I. Honma, and H. Zhou, *Electrochem. Commun.*, **8**, 284 (2006).
12. E. Hosono, S. Fujihara, I. Honma, and H. Zhou, *J. Electrochem. Soc.*, **153**, A1273 (2006).
13. T. Kudo, Y. Ikeda, T. Watanabe, M. Hibino, M. Miyayama, H. Abe, and K. Kajita, *Solid State Ionics*, **152–153**, 833 (2002).
14. I. Moriguchi, R. Hidaka, H. Yamada, T. Kudo, H. Murakami, and N. Nakashima, *Adv. Mater. (Weinheim, Ger.)*, **18**, 69 (2006).
15. H. Zhou, D. Li, M. Hibino, and I. Honma, *Angew. Chem., Int. Ed.*, **44**, 797 (2005).
16. J. Wang, I. D. Raistrick, and R. A. Huggins, *J. Electrochem. Soc.*, **133**, 457 (1986).
17. Z. W. Fu and Q. Z. Qin, *J. Phys. Chem. B*, **104**, 5505 (2000).
18. H. C. Shin, J. Dong, and M. Liu, *Adv. Mater. (Weinheim, Ger.)*, **15**, 1610 (2003).
19. H. C. Shin and M. Liu, *Adv. Funct. Mater.*, **15**, 582 (2005).